nature sustainability

Article

https://doi.org/10.1038/s41893-022-00976-8

# Socio-demographic factors shaping the future global health burden from air pollution

In the format provided by the authors and unedited

**Supplementary Information for "*Socio-demographic factors shaping the future global health burden from air pollution*"**

*Hui Yang, Xinyuan Huang, Daniel M. Westervelt, Larry Horowitz, Wei Peng (weipeng@psu.edu)*

This supplementary information appendix includes the following information:

## 1. Additional information on method

### 1.1 Supplemental Note 1: SSP-RCP scenario framework

Based on projections on energy use, land use and emissions of air pollutants and greenhouse gases (GHGs), the SSP-RCP scenario framework pioneers a process of developing scenarios for socioeconomic narratives and global warming levels.[1] The Shared Socioeconomic Pathways (SSPs) narrate possible alternative trends in socioeconomic and environmental development.[2] As described by Gidden et al. (2019),[3] the five SSPs, as in narratives[2] and model quantifications,[4–8] characterize features of potential futures in which the world follows business as usual (SSP2), socioeconomic and technological development are renewables or fossil-fueled (SSP1/SSP5), or resources are unequally distributed between or within countries (SSP3/SSP4). Each pathway pertains to different levels of socioeconomic challenges to climate change mitigation and adaptation. The distinct differences across the SSPs are driven by the basic SSP elements which are population, urbanization, and GDP.[9] In addition, each Representative Concentration Pathway represents the warming targets for the emission pathways of energy system and land use, as measured as certain radiative forcing levels (in $W/m^2$) by the end of the century.[1] Four RCPs are introduced in IPCC AR5 report,[10] which are the low-emission scenario RCP2.6,[11] stabilization scenario RCP4.5,[12] climate-policy intervention scenario RCP6.0,[13] and no-mitigation scenario RCP8.5.[14] They are in line with a wide range of plausible changes in future anthropogenic greenhouse gas emissions. Based on the CMIP5 ensembles,[15] the respective scenarios are projected to lead to 1.0 °C (0.3 °C to 1.7 °C), 1.8 °C (1.1 °C to 2.6 °C), 2.2 °C (1.4 °C to 3.1 °C), and 3.7 °C (2.6 °C to 4.8 °C) of global mean temperature increase in the late 21$^{st}$ century relative to the reference period (1986–2005).[10] The combination of SSPs and RCPs are introduced based on the Shared Climate Policy Assumptions which comprise of information such as the evolution of global climate policies and long-term target for climate mitigation. The definition of this integrated scenario architecture intends to capture the central features of climate policies globally through the end of the century.[16]

The SSP-RCP scenario framework has been widely adopted across research communities in scientific assessments such as CMIP6[17] and the IPCC AR6 report.[18] CMIP6 seeks to better understand the response of the Earth system to climate forcing, systematic biases of the Earth system and climate models, and assessment of future climate change in scenarios. It also offers an opportunity for studying air pollutant trajectories as well as the changes in air quality and health impacts under various plausible future pathways.[17] As a major component of CMIP6, the Scenario Model Intercomparison Project (ScenarioMIP)[19] serves as the basis for other CMIP6-endorsed MIPs and provides a greater level of understanding on physical and social impacts of future climate. Climate projections are simulated by multiple models and each model conducts simulations for a selection of SSP-RCP scenarios. Since ScenarioMIP focuses on emissions-driven simulations, for each scenario, the emissions input are gridded datasets comprising historical and future (2015 to 2100) emissions, which include anthropogenic and open burning emissions.[20] The gridded future anthropogenic emissions data is derived from the future emissions trajectory by Gidden et al. (2019).[3]

The set of scenarios considered in ScenarioMIP is categorized into Tier 1 and Tier 2 scenarios. Tier 1 scenarios span the climate forcing target levels similar to the RCPs adopted in CMIP5. Tier 2 scenarios include additional add-ons beyond those scenarios in CMIP5[3] and allow us to study the roles of different factors.

Figure S1 shows the five SSP-RCP scenarios used in this study, in line with the emissions scenarios in the IPCC AR6 report.[18] The end-of-century warming levels of these scenarios range from a lower bound of 1.9 W/m$^2$ (below 2°C) to an upper bound of 8.5 W/m$^2$ (nearly 5°C) of end-of-century warming level.[3] These scenarios are also subject to different levels of air pollution emissions consistent with different SSP storylines.[21] Specifically, SSP1-1.9, SSP1-2.6, and SSP5-8.5 describe the plausible futures with high economic development (via sustainable energy or fossil fuel use) and strong pollution control, while SSP3-7.0 has the highest air pollutant emissions.[22]

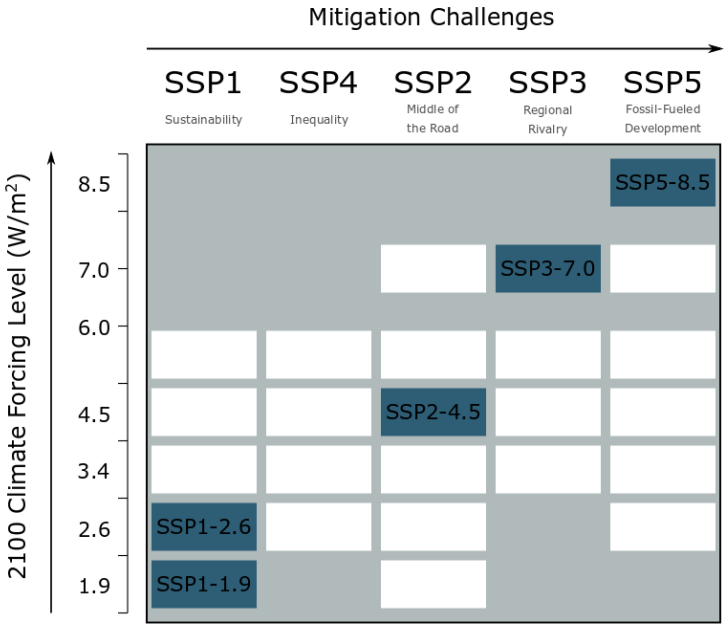


Figure S1. The SSP-RCP scenarios in this study, outlined in dark blue. The matrix here illustrates the coupled SSP-RCP scenario framework, with SSP (i.e., socioeconomic development) as the x-axis and RCP (i.e., climate forcing target) as the y-axis. Each cell in the matrix indicates an SSP-RCP scenario that is shown to be practicable from Integrated Assessment Model (IAM) runs. We reproduced this figure based on Riahi et al. (2017).[9]

### 1.2 Supplemental Note 2: GFDL-ESM4.1 model evaluation

The performance of the GFDL-ESM4.1 model to simulate ambient $PM_{2.5}$ concentrations has been evaluated in prior publications.[23–25]

#### (a) $PM_{2.5}$ concentrations

Turnock et al. (2020)[25] evaluated the model performance for all CMIP6 models, including results from ESM4.1 that are being used in this study. The study compared the simulated and observed

$PM_{2.5}$ concentrations for all the locations in the database of the Global Aerosol Synthesis and Science Project (GASSP; http://gassp.org.uk/data/). For background, non-urban $PM_{2.5}$, it obtained observations from three major networks: (1) the Interagency Monitoring of Protected Visual Environment (IMPROVE) network in North America, (2) the European Monitoring and Evaluation Progamme (EMEP), and (2) Asia-Pacific Aerosole Database (A-PAD). Besides monitoring data, a further comparison was made with the Modern-Era Retrospective Analysis for Research and Applications, version 2 (MERRA-2) aerosol reanalysis product. The summary of the multi-model evaluation results were reported in Section 3.2 of the paper, with specific results for GFDL-ESM4.1 model included in their Supplemental Materials.

**(b) Aerosol components**

Horowitz et al. (2020)[24] evaluated the performance of AM4.1, the atmospheric component of GFDL-ESM4.1 that is used to simulate $PM_{2.5}$ in this study. The key model evaluation results are reported in Section 4.3 of this paper.

In short, simulated nitrate and sulfate aerosols were compared with observations from the IMPROVE network.[26–28] The IMPROVE network is designed to monitor spatial and temporal trends of visibility-reducing particulate matter pollution for more than 170 sites across the US; it collects 24-hour samples every three days.[26–28] The simulated nitrate concentrations were found to correlate well with the observations (R = 0.74) with a bias towards the high end (normalized mean bias [NMB] = +80%). Sulfate simulations successfully captured the wide range of sulfate aerosol concentrations in the observational data across regions. The concentrations of nitrate and sulfate in precipitation were evaluated against the observations from the NADP (National Atmospheric Deposition Program) network, which monitors precipitation chemistry weekly at 390 sites across North America.[29] The simulated results were well correlated with the observations, with a high bias for nitrate (NMB = +35%) and a low bias for sulfate (NMB = -19%).

Simulated aerosol optical depths (AOD) from AM4.1 were also compared with the measurements from the AERONET (Aerosol Robotic Network), the largest, worldwide sun photometer network that collects daily measurement data for more than 600 sites around the world.[30,31] Comparing the simulated and observed data, the correlation was high (0.9) and the root mean square was low (0.08). In particular, compared to earlier versions of the model, AM4.1 simulations exhibited a large reduction in positive bias in the tropics and equatorial regions, which demonstrated the more efficient aerosol removal by convective precipitation that is captured in the new version.

**1.3 Baseline mortality rates**

Table S1. Baseline mortality rates of six diseases in 2015 (unit: deaths per million people). We compared the estimates from GBD 2019[32] and the estimates based on our mapping methods based on IF projections.[33] More details can be found in the Method section in the main text. The lower bound (LB) and upper bound (UB) represent the 95% confidence interval based on the relative risk functions.

| | GBD 2019 | | | Our estimates based on IF |
|---|---|---|---|---|
| | Central Value | Lower bound | Upper bound | |
| Ischemic heart disease (IHD) | 2033 | 1895 | 2184 | 1945 |
| Stroke | 1392 | 1266 | 1508 | 1319 |
| Chronic obstructive pulmonary disease (COPD) | 718 | 630 | 819 | 640 |
| Lower respiratory tract infection (LRI) | 377 | 319 | 443 | 265 |
| Lung cancer | 424 | 393 | 459 | 407 |
| Type-2 diabetes | 226 | 195 | 262 | 218 |

## 2. Additional results

### 2.1 Cumulative carbon emissions and cumulative deaths from 2015 to 2050

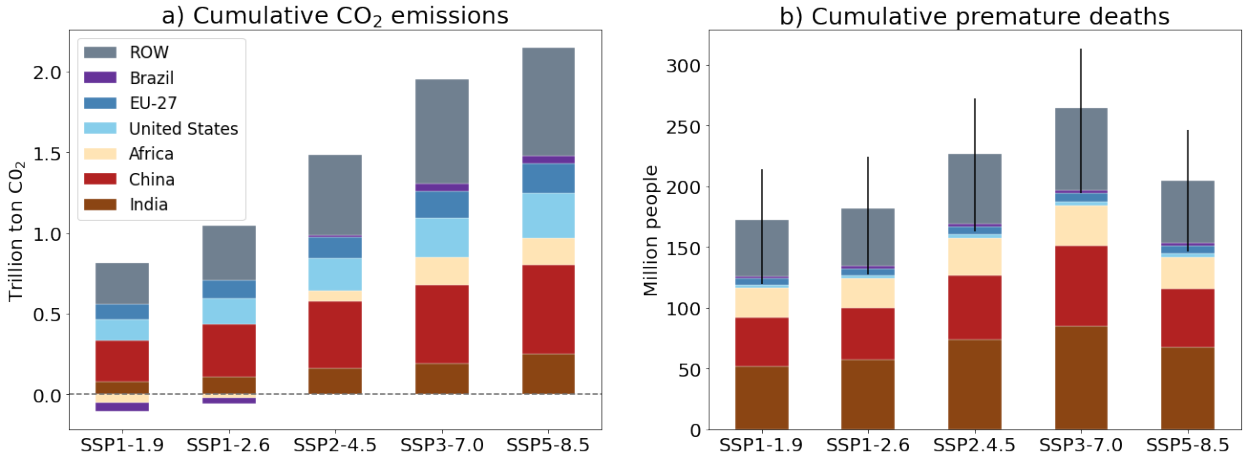


Figure S2. Cumulative $CO_2$ emissions (left panel) and $PM_{2.5}$-related premature deaths (right panel) from 2015 to 2050 in the five SSP-RCP scenarios. Different colors represent different world regions (ROW: rest of the world). The error bars in panel b) represent the deaths estimated based on the 95% confidence interval of the relative risk functions from the Global Burden of Disease Study.[34,35]

### 2.2 Global average temperature projected by GFDL-ESM4.1

Table S2. Changes in global average temperature relative to preindustrial times (1850-1900) based on our GFDL-ESM4.1 projections.

| | Near term (2021-2040) | Mid-term (2041-2060) | Long term (2081-2100) |
|---|---|---|---|
| SSP1-1.9 | 1.37°C | 1.39°C | 1.16°C |

| | | | |
|---|---|---|---|
| SSP1-2.6 | 1.28°C | 1.48°C | 1.49°C |
| SSP2-4.5 | 1.34°C | 1.68°C | 2.34°C |
| SSP3-7.0 | 1.32°C | 1.89°C | 3.40°C |
| SSP5-8.5 | 1.39°C | 2.06°C | 3.90°C |

### 2.3 Gridded temperature projections by GFDL-ESM4.1

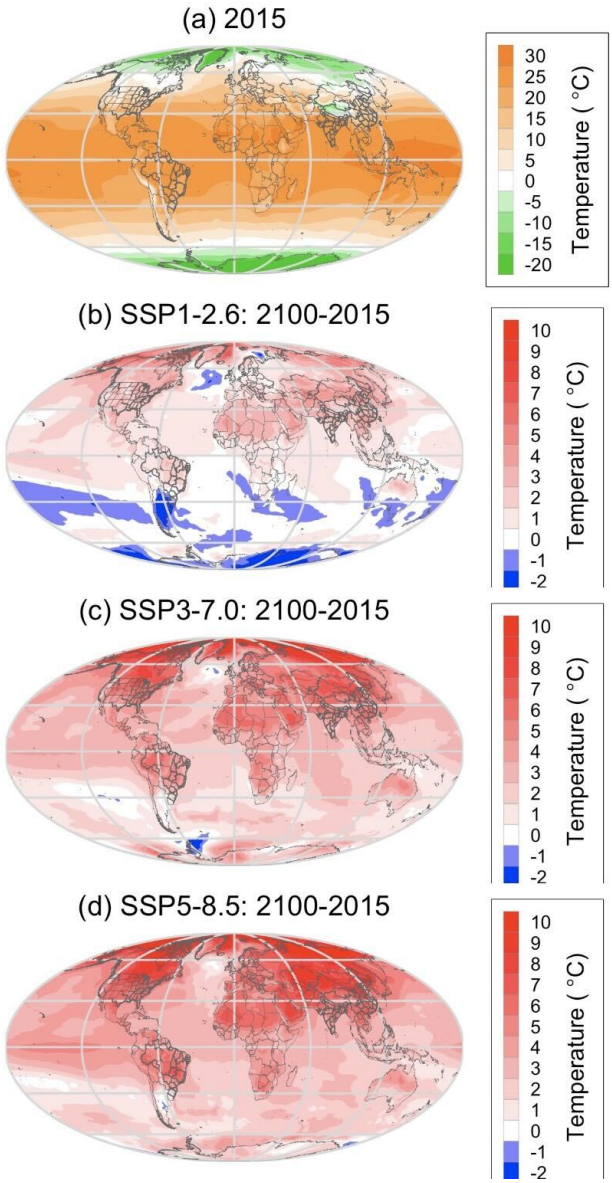


Figure S3. Global temperature projections by GFDL-ESM4.1.[23,36] Panel a) shows the global annual mean temperature in 2015. Panels b)-d) show the differences in 2100 as compared to 2015 for SSP1-2.6, SSP3-7.0, and SSP5-8.5.

## 2.4 Global premature deaths by age and country income group

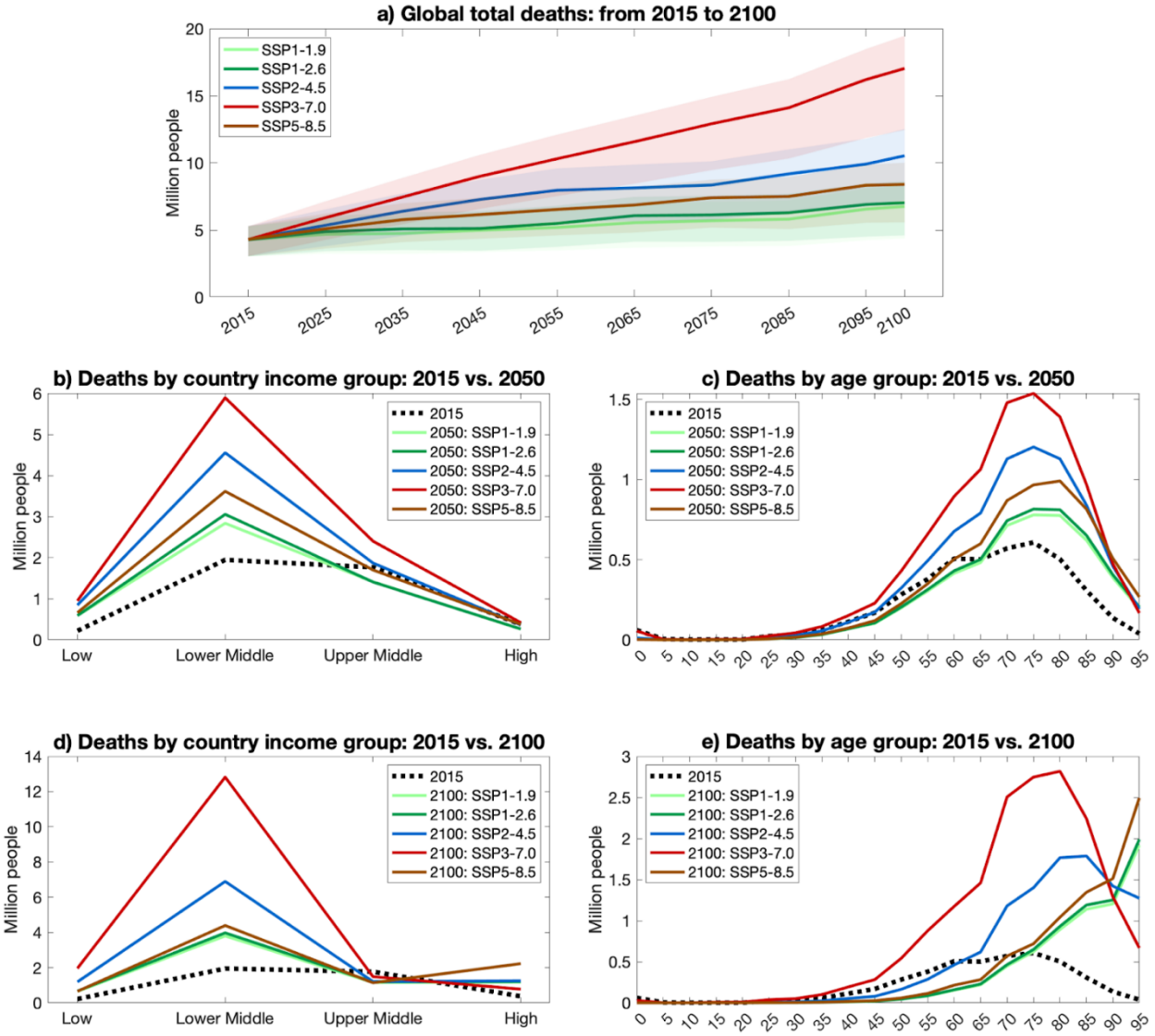


Figure S4. Global total deaths from ambient $PM_{2.5}$ exposure and the distribution of health burden across regions and age groups. Panel a): Global total annual deaths from 2015 to 2100. The lines and the shades show the calculated $PM_{2.5}$-related deaths based on the central estimate and the 95% confidence intervals of the relative risk functions from GBD 2019.[34] Panel b) and d): Deaths by country income groups in 2015, 2050, and 2100 based on the central estimates of the relative risk functions; here we use the World Bank country classification.[37] Panel c) and e): Global total deaths from ambient $PM_{2.5}$ exposure by age group in 2015, 2050, and 2100 based on the central estimates of the relative risk functions; here the x-axis label shows the start age of each of the five-year age groups.

## 2.5 Global distribution of simulated $PM_{2.5}$ concentrations and premature deaths for SSP1-1.9 and SSP2-4.5 at the end of the century

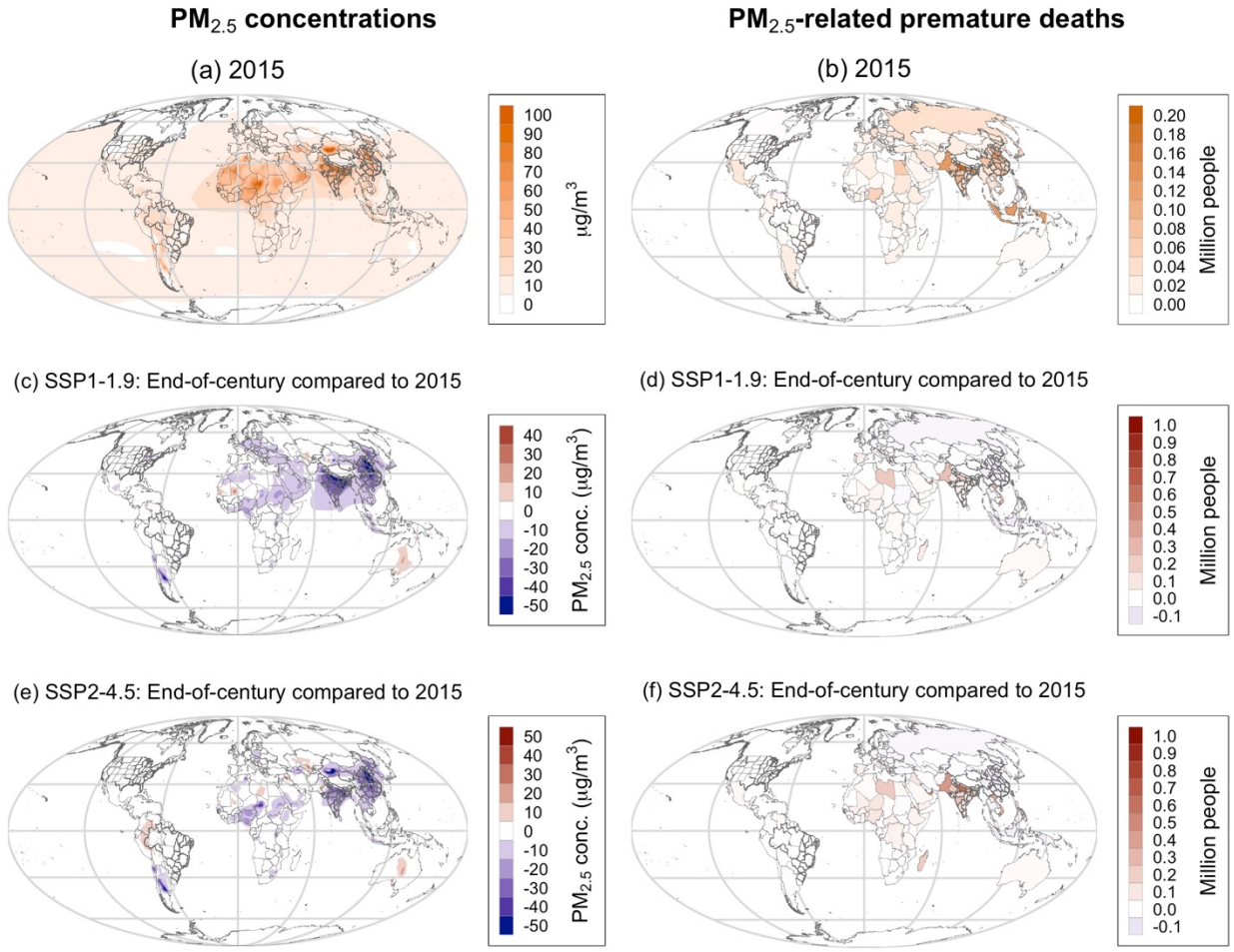


Figure S5. Global distribution of annual mean $PM_{2.5}$ concentrations (left column) and annual total premature deaths (right column) in 2015 and the end of century for SSP1-1.9 and SSP2-4.5. Panels a) and b) show the patterns in 2015. Panels c)-f) show the differences in the end of the century as compared to 2015. The $PM_{2.5}$ concentrations are at 1° latitude by 1.25° longitude resolution. The end-of-century values are calculated using the multi-year averages from a selected time horizon (2090-2100).

## 2.6 Global distribution of simulated $PM_{2.5}$ concentrations and premature deaths for 2050

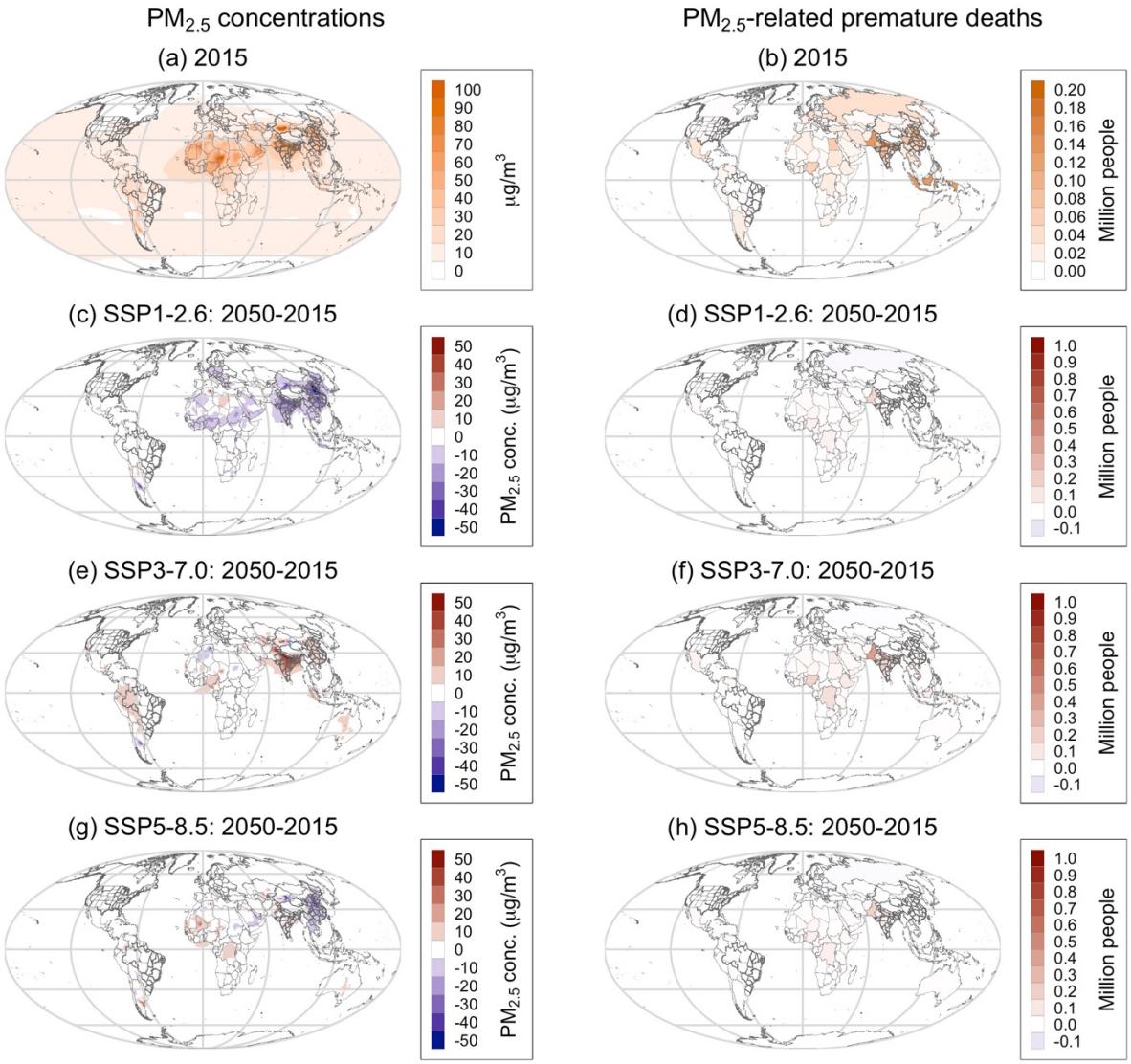


Figure S6. Global distribution of annual mean $PM_{2.5}$ concentrations (left column) and annual total premature deaths (right column) in 2015 and 2050 for SSP1-2.6, SSP3-7.0 and SSP5-8.5. Panels a) and b) show the patterns in 2015. Panels c)-h) show the differences in 2050 as compared to 2015.

### 2.7 Global distribution of $PM_{2.5}$-related death rate

While the premature deaths measure the total health burden, the $PM_{2.5}$-related death rates (i.e., deaths divided by population) measure the level of risk facing the populations. Here we show the global distribution of $PM_{2.5}$-related death rates in Figure S7 (mid-century) and S8 (end-of-century), as an alternative metric to measure the health impacts.

In all scenarios, we find the Global South countries suffer from higher risk at present and in future time periods. In addition, the lower-income regions, such as India and regions in Africa and Southeast Asia, are expected to experience greater increases in $PM_{2.5}$-related death rates in the future. Such result is largely driven by higher pollution levels in these regions combined with higher baseline mortality rates. It highlights the importance of sociodemographic factors in determining the population vulnerability and mortality risks from $PM_{2.5}$ exposure.

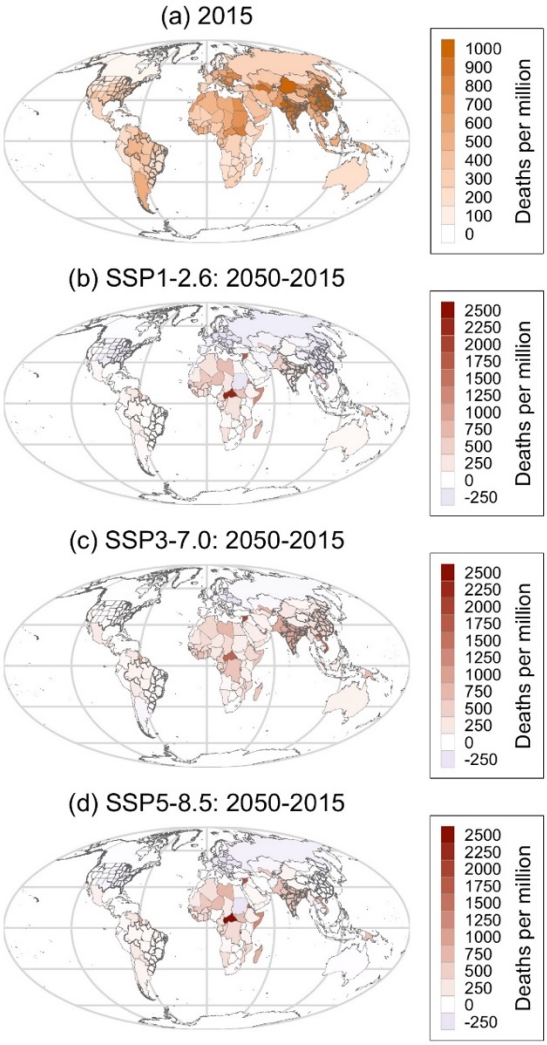


Figure S7. Global distribution of $PM_{2.5}$-related premature death rate in 2015 and 2050 for SSP1-2.6, SSP3-7.0 and SSP5-8.5. Panel a) shows the patterns in 2015. Panels b)-d) show the differences in 2050 as compared to 2015.

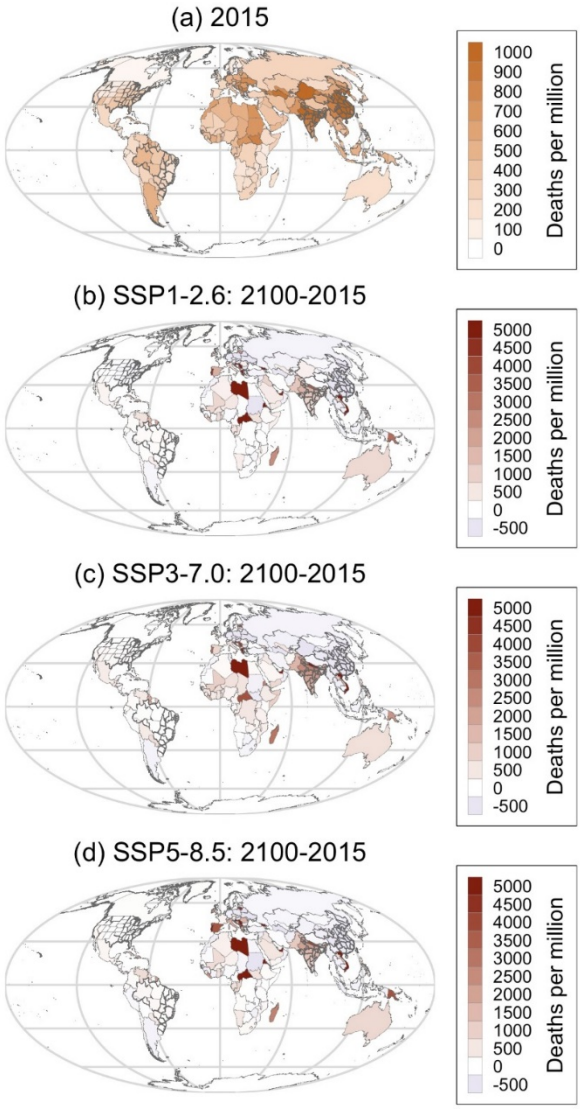


Figure S8. Global distribution of $PM_{2.5}$-related premature death rate in 2015 and the end of the century for SSP1-2.6, SSP3-7.0 and SSP5-8.5. Panel a) and b) show the patterns in 2015. Panels c)-h) show the differences in 2100 as compared to 2015.

## 2.8 Decomposition analysis for all five scenarios for 2050 and 2100

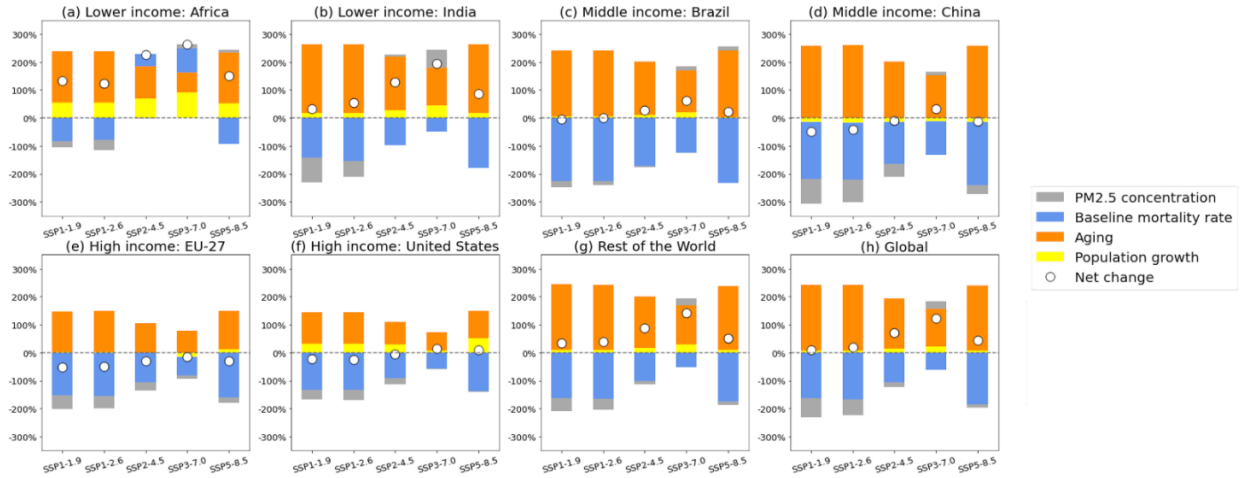


Figure S9. Relative contribution of four individual factors to the 2015-2050 changes in $PM_{2.5}$-related deaths: changes in $PM_{2.5}$ concentrations (grey), baseline mortality rate (blue), population ageing (orange), and population growth (yellow). Combining the effects of these four factors, the white dots represent the net changes in 2050 relative to 2015.

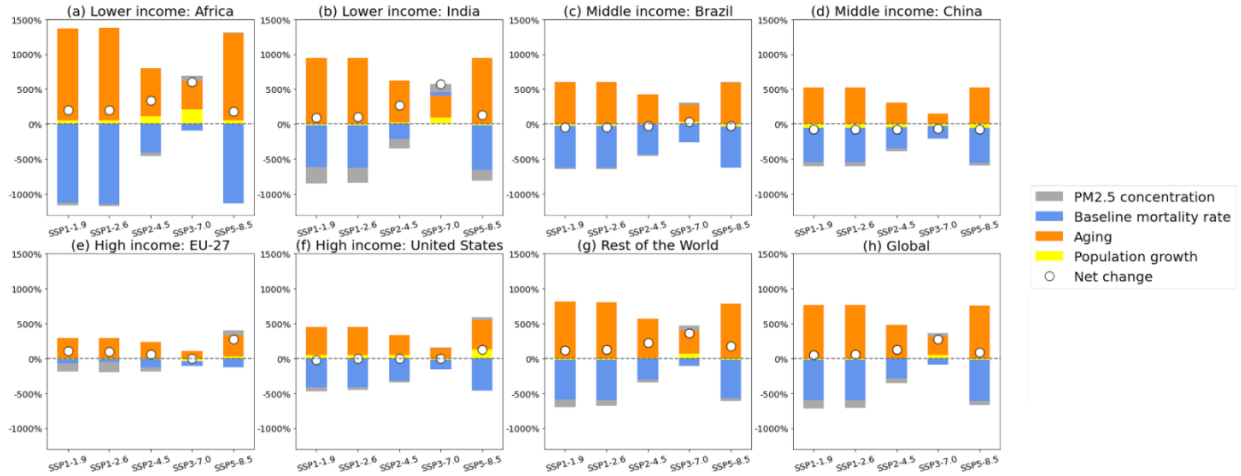


Figure S10. Relative contribution of four individual factors to the 2015-2100 changes in $PM_{2.5}$-related deaths: changes in $PM_{2.5}$ concentrations (grey), baseline mortality rate (blue), population ageing (orange) and population growth (yellow). Combining the effects of these four factors, the white dots represent the net changes in 2100 relative to 2015.

## 3. Sensitivity analysis for health impact assessment

### 3.1 Relative risk functions

While our main results use the relative risk functions from the Global Burden of Disease (GBD) 2019[34,35], as a sensitivity analysis, here we compare the alternative RR estimates from GBD 2017[38,39], as well as the Global Exposure Mortality Model (GEMM) study.[40]

Compared to GBD 2017, GBD 2019 includes new data from 44 cohort studies. The newly added data and changes in fitting the dose-response curves contribute to higher RR estimates for cardiovascular diseases, especially stroke.

Compared to GBD (specifically, the integrated exposure-response (IER) model from GBD 2015),[41] GEMM solely relies on the studies of outdoor $PM_{2.5}$. Hence, the RR estimates from GEMM are almost always greater than those from the previous IER model, with much higher risks observed at higher $PM_{2.5}$ concentrations. Note that compared to GBD estimates, GEMM does not report RRs for type 2 diabetes, which affects the comparison for the aggregate deaths.

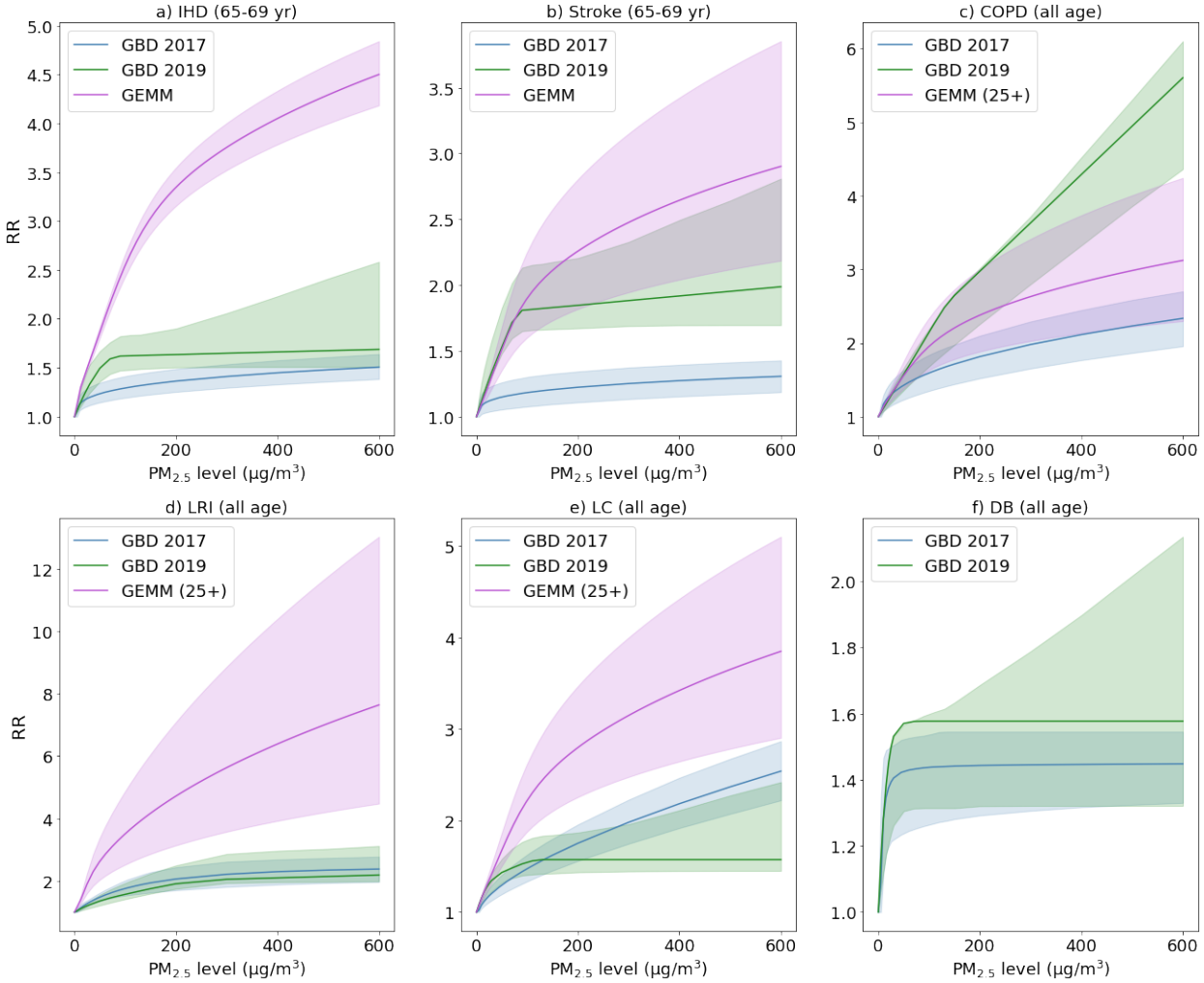


Figure S11. Relative risk (RR) curves from different sources for six diseases – (a) ischemic heart disease (IHD), (b) Stroke, (c) chronic obstructive pulmonary disease (COPD), (d) lower respiratory tract infection (LRI), (e) lung cancer and (f) type-2 diabetes. For IHD and Stroke we present the RR for the age group of 65-69 years old; for COPD, LRI, LC, and DB the RR relationships are for all ages. For panels c) – e), as indicated in the legends, the GEMM concentration response functions are only for people above the age of 25, while GBD functions are for all ages. For panel f), only GBD RR curves are shown since GEMM does not report RR for diabetes type 2. In all panels, the error bars represent 95% confidence interval for the RR functions. The solid lines represent the central estimates of the RR values reported from each source.

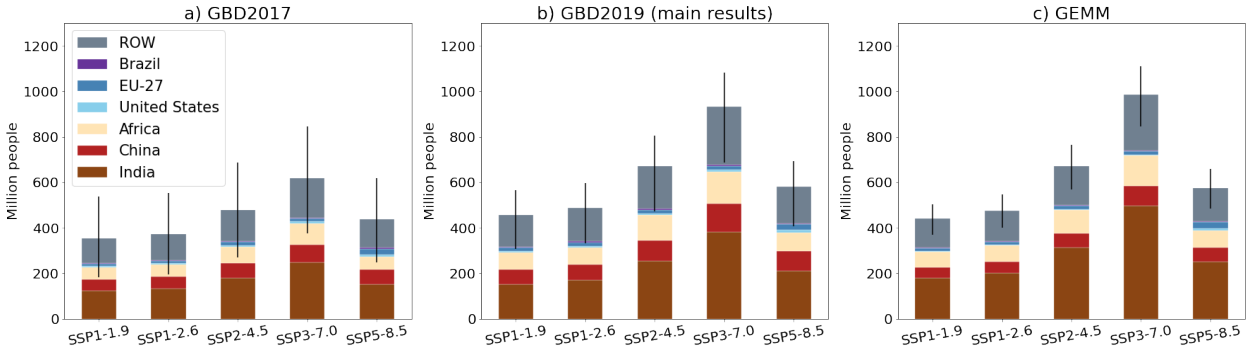


Figure S12. Cumulative global $PM_{2.5}$-related deaths from 2015 to 2100 using different relative risk functions: (a) GBD 2017[38,39] (as sensitivity analysis), (b) GBD 2019[34,35] (our main method; same as Figure 2 in the main text) and (c) GEMM[42] (as sensitivity analysis) relative risk functions. Different colors represent different world regions (ROW: rest of the world). The bars in panel a), b) and c) represent the results using the central estimates of the relative risk functions from the Global Burden of Disease Study[34,43] and the Global Exposure Mortality Model,[42] whereas the error bars represent the deaths estimated based on the 95% confidence interval of the relative risk functions. Note that the GEMM estimates do not include the deaths from diabetes type 2.

### 3.2 Years of life lost

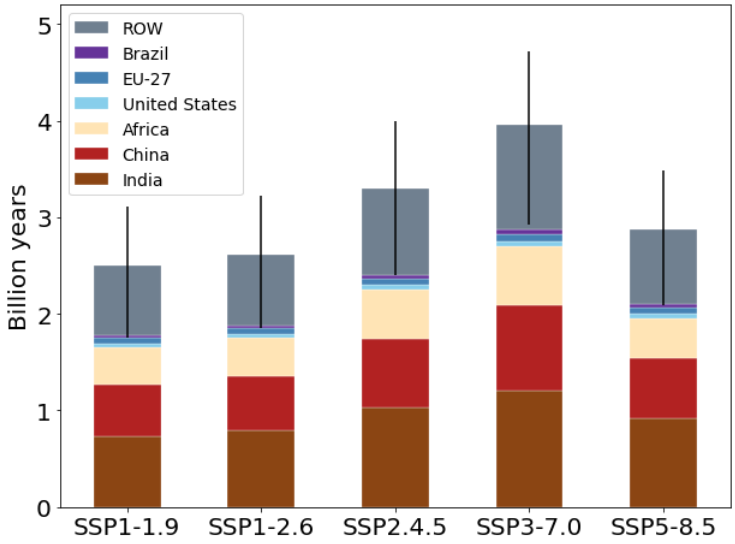


Figure S13. Cumulative global $PM_{2.5}$-related years of life lost from 2015 to 2050 calculated using GBD 2019[34,35] relative risk functions. The bars represent the results using the central estimates, whereas the error bars represent the deaths estimated based on the 95% confidence interval of the relative risk functions from the Global Burden of Disease Study.[34] Years of life lost (YLL) is calculated from: $\Delta\mathrm{YLL} = \Delta\mathrm{Mort} \times \mathrm{YLL}_0$, where $\mathrm{YLL}_0$ is the baseline years of life lost (i.e., life expectancy at a certain age). $\mathrm{YLL}_0$ is adopted from the GBD 2017 abridged life tables[44] by country and age group at five-year intervals. Since life expectancy can also change with socioeconomic development and the availability of health care resources, future work should consider projecting evolving life expectancy over time, instead of assuming it stays constant at the present-level level.

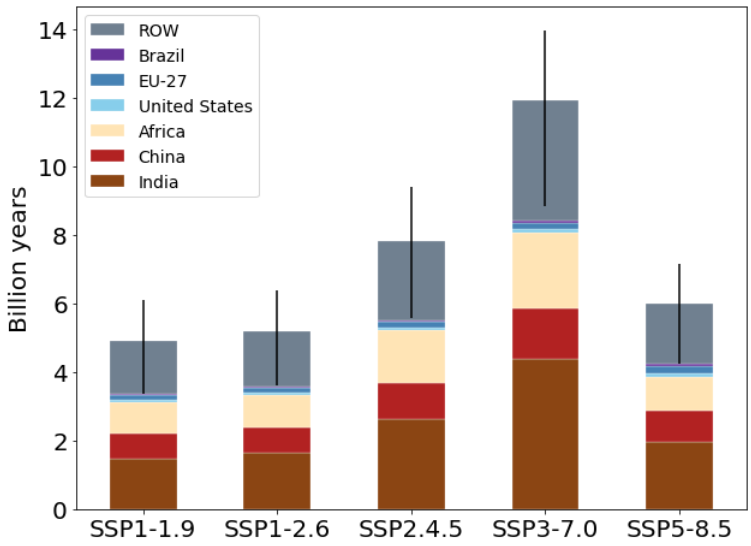


Figure S14. Cumulative global $PM_{2.5}$-related years of life lost from 2015 to 2100 calculated using GBD 2019[34,35] relative risk functions. The bars represent the results using the central estimates, whereas the error bars represent the deaths estimated based on the 95% confidence interval of the relative risk functions from the Global Burden of Disease Study.[34]

**Reference**


1. van Vuuren, D. P. *et al.* The representative concentration pathways: An overview. *Clim. Change* (2011) doi:10.1007/s10584-011-0148-z.
2. O'Neill, B. C. *et al.* A new scenario framework for climate change research: The concept of shared socioeconomic pathways. *Clim. Change* (2014) doi:10.1007/s10584-013-0905-2.
3. Gidden, M. J. *et al.* Global emissions pathways under different socioeconomic scenarios for use in CMIP6: A dataset of harmonized emissions trajectories through the end of the century. *Geosci. Model Dev.* (2019) doi:10.5194/gmd-12-1443-2019.
4. Calvin, K. *et al.* The SSP4: A world of deepening inequality. *Glob. Environ. Chang.* (2017) doi:10.1016/j.gloenvcha.2016.06.010.
5. Fricko, O. *et al.* The marker quantification of the Shared Socioeconomic Pathway 2: A middle-of-the-road scenario for the 21st century. *Glob. Environ. Chang.* (2017) doi:10.1016/j.gloenvcha.2016.06.004.
6. Fujimori, S. *et al.* SSP3: AIM implementation of Shared Socioeconomic Pathways. *Glob. Environ. Chang.* (2017) doi:10.1016/j.gloenvcha.2016.06.009.
7. Kriegler, E. *et al.* Fossil-fueled development (SSP5): An energy and resource intensive scenario for the 21st century. *Glob. Environ. Chang.* (2017) doi:10.1016/j.gloenvcha.2016.05.015.
8. van Vuuren, D. P. *et al.* Energy, land-use and greenhouse gas emissions trajectories under a green growth paradigm. *Glob. Environ. Chang.* (2017) doi:10.1016/j.gloenvcha.2016.05.008.
9. Riahi, K. *et al.* The Shared Socioeconomic Pathways and their energy, land use, and greenhouse gas emissions implications: An overview. *Glob. Environ. Chang.* (2017) doi:10.1016/j.gloenvcha.2016.05.009.
10. IPCC. *Summary for Policymakers. In: Climate Change 2013: The Physical Science Basis. Contribution of Working Group I to the Fifth Assessment Report of the Intergovernmental Panel on Climate Change*. https://www.ipcc.ch/site/assets/uploads/2018/02/WG1AR5_SPM_FINAL.pdf (2013).
11. van Vuuren, D. P. *et al.* RCP2.6: Exploring the possibility to keep global mean temperature increase below 2°C. *Clim. Change* (2011) doi:10.1007/s10584-011-0152-3.
12. Thomson, A. M. *et al.* RCP4.5: A pathway for stabilization of radiative forcing by 2100. *Clim. Change* (2011) doi:10.1007/s10584-011-0151-4.
13. Masui, T. *et al.* An emission pathway for stabilization at 6 Wm-2 radiative forcing. *Clim. Change* (2011) doi:10.1007/s10584-011-0150-5.
14. Riahi, K. *et al.* RCP 8.5-A scenario of comparatively high greenhouse gas emissions. *Clim. Change* (2011) doi:10.1007/s10584-011-0149-y.
15. Taylor, K. E., Stouffer, R. J. & Meehl, G. A. An overview of CMIP5 and the experiment design. *Bulletin of the American Meteorological Society* (2012) doi:10.1175/BAMS-D-11-00094.1.
16. Kriegler, E. *et al.* A new scenario framework for climate change research: The concept of shared climate policy assumptions. *Clim. Change* (2014) doi:10.1007/s10584-013-0971-5.
17. Eyring, V. *et al.* Overview of the Coupled Model Intercomparison Project Phase 6 (CMIP6) experimental design and organization. *Geosci. Model Dev.* (2016) doi:10.5194/gmd-9-1937-2016.
18. IPCC. *Summary for Policymakers. In: Climate Change 2021: The Physical Science Basis. Contribution of Working Group I to the Sixth Assessment Report of the Intergovernmental Panel on Climate Change*. http://web.archive.org/web/20210819125401/https://www.ipcc.ch/report/ar6/wg1/downloads/report/IPCC_AR6_WGI_SPM.pdf (2021).
19. O'Neill, B. C. *et al.* The Scenario Model Intercomparison Project (ScenarioMIP) for CMIP6.

*Geosci. Model Dev.* (2016) doi:10.5194/gmd-9-3461-2016.
20. Feng, L. *et al.* The generation of gridded emissions data for CMIP6. *Geosci. Model Dev.* (2020) doi:10.5194/gmd-13-461-2020.
21. Rao, S. *et al.* Future air pollution in the Shared Socio-economic Pathways. *Glob. Environ. Chang.* (2017) doi:10.1016/j.gloenvcha.2016.05.012.
22. Collins, J. W. *et al.* AerChemMIP: Quantifying the effects of chemistry and aerosols in CMIP6. *Geosci. Model Dev.* (2017) doi:10.5194/gmd-10-585-2017.
23. Dunne, J. P. *et al.* The GFDL Earth System Model Version 4.1 (GFDL-ESM 4.1): Overall Coupled Model Description and Simulation Characteristics. *J. Adv. Model. Earth Syst.* (2020) doi:10.1029/2019MS002015.
24. Horowitz, L. W. *et al.* The GFDL Global Atmospheric Chemistry-Climate Model AM4.1: Model Description and Simulation Characteristics. *J. Adv. Model. Earth Syst.* (2020) doi:10.1029/2019MS002032.
25. Turnock, S. T. *et al.* Historical and future changes in air pollutants from CMIP6 models. *Atmos. Chem. Phys.* (2020) doi:10.5194/acp-20-1$^{45}$47-2020.
26. Hyslop, N. P. IMPROVE Aerosol Measurements: Overview and Updates. https://www.epa.gov/sites/default/files/2016-10/documents/aerosol_measurements.pdf (2016).
27. Malm, W. C., Sisler, J. F., Huffman, D., Eldred, R. A. & Cahill, T. A. Spatial and seasonal trends in particle concentration and optical extinction in the United States. *J. Geophys. Res.* (1994) doi:10.1029/93JD02916.
28. Jongeward, A. R., Li, Z., He, H. & Xiong, X. Natural and anthropogenic aerosol trends from satellite and surface observations and model simulations over the North Atlantic Ocean from 2002 to 2012. *J. Atmos. Sci.* (2016) doi:10.1175/JAS-D-15-0308.1.
29. Water Resources. National Atmospheric Deposition Program (NADP). https://www.usgs.gov/mission-areas/water-resources/science/national-atmospheric-deposition-program-nadp (2021).
30. Giles, D. M. *et al.* Advancements in the Aerosol Robotic Network (AERONET) Version 3 database - Automated near-real-time quality control algorithm with improved cloud screening for Sun photometer aerosol optical depth (AOD) measurements. *Atmos. Meas. Tech.* (2019) doi:10.5194/amt-12-169-2019.
31. Holben, B. N. *et al.* AERONET - A federated instrument network and data archive for aerosol characterization. *Remote Sens. Environ.* (1998) doi:10.1016/S0034-4257(98)00031-5.
32. Global Burden of Disease Collaborative Network. Global Burden of Disease Study 2019 (GBD 2019) Under-5 Mortality and Adult Mortality 1950-2019. https://ghdx.healthdata.org/record/ihme-data/gbd-2019-mortality-estimates-1950-2019 (2020).
33. International Futures (IFs) modeling system, V. 7. 45. Frederick S. Pardee Center for International Futures, Josef Korbel School of International Studies, University of Denver, Denver, CO. https://pardee.du.edu/access-ifs (2020).
34. Murray, C. L. *et al.* Global burden of 87 risk factors in 204 countries and territories, 1990-2019: a systematic analysis for the Global Burden of Disease Study 2019. *Lancet* (2020).
35. Global Burden of Disease Collaborative Network. Global Burden of Disease Study 2019 (GBD 2019) Burden by Risk 1990-2019. http://ghdx.healthdata.org/record/ihme-data/gbd-2019-burden-by-risk-1990-2019 (2020).
36. John, J. G. *et al.* NOAA-GFDL GFDL-ESM4 model output prepared for CMIP6 ScenarioMIP. Version 20180701. *Earth System Grid Federation* https://doi.org/10.22033/ESGF/CMIP6.1414 (2018).
37. The World Bank. World Bank Country and Lending Groups. https://datahelpdesk.worldbank.org/knowledgebase/articles/906519-world-bank-country-

and-lending-groups (2020).
38. Global Burden of Disease Collaborative Network. Global Burden of Disease Study 2017 (GBD 2017) Burden by Risk 1990-2017. http://ghdx.healthdata.org/record/ihme-data/gbd-2017-burden-risk-1990-2017 (2018).
39. Stanaway, J. D. *et al.* Global, regional, and national comparative risk assessment of 84 behavioural, environmental and occupational, and metabolic risks or clusters of risks for 195 countries and territories, 1990-2017: A systematic analysis for the Global Burden of Disease Stu. *Lancet* (2018) doi:10.1016/S0140-6736(18)32225-6.
40. Burnett, R. *et al.* Global estimates of mortality associated with longterm exposure to outdoor fine particulate matter. *Proc. Natl. Acad. Sci. U. S. A.* (2018) doi:10.1073/pnas.1803222115.
41. Burnett, R. T. *et al.* An integrated risk function for estimating the global burden of disease attributable to ambient fine particulate matter exposure. *Environ. Health Perspect.* (2014) doi:10.1289/ehp.1307049.
42. Burnett, R. *et al.* Global estimates of mortality associated with longterm exposure to outdoor fine particulate matter. *Proc. Natl. Acad. Sci. U. S. A.* (2018) doi:10.1073/pnas.1803222115.
43. Stanaway, J. D. *et al.* Global, regional, and national comparative risk assessment of 84 behavioural, environmental and occupational, and metabolic risks or clusters of risks for 195 countries and territories, 1990-2017: A systematic analysis for the Global Burden of Disease Stu. *Lancet* (2018) doi:10.1016/S0140-6736(18)32225-6.
44. Global Burden of Disease Collaborative Network. Global Burden of Disease Study 2017 (GBD 2017) Life Tables 1950-2017. https://ghdx.healthdata.org/record/ihme-data/gbd-2017-life-tables-1950-2017 (2018).